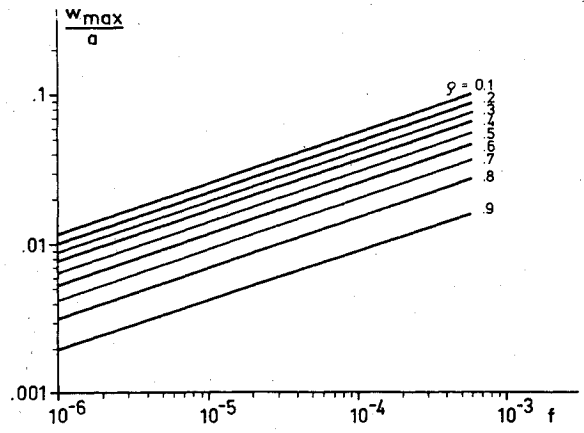

Fig. 4 Maximum deflection vs loading magnitude.

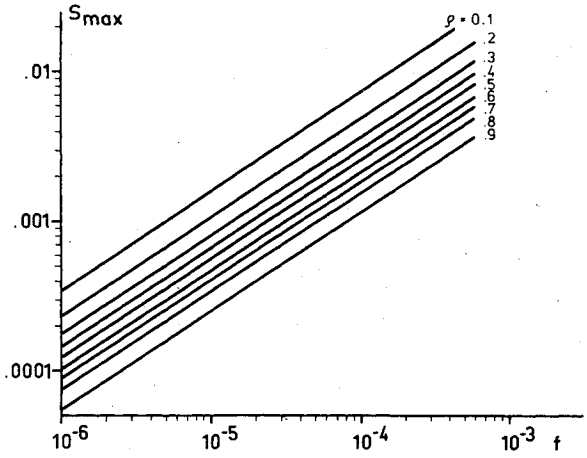

Fig. 5 Maximum stress vs loading magnitude.

$$s_0=(f/\rho\varphi_0) \qquad t_0=\nu s_0$$

By means of Eqs. (9a) and (10a), the nondimensional stresses s and t are then determined for radial locations between $\rho=1$ and $\rho=\rho_1$, and at the latter location, the boundary condition is checked. A corrected value of φ_0 is then chosen and the computation repeated until the correct boundary condition is obtained. This calculation has been carried out for a range of values of the parameters f and ρ_1, employing a Kutta-Merson procedure coded in APL, with a Burroughs computer (Table 1).

The necessary condition of small slope does not occur at small values of ρ_1. This is equivalent to approaching a point load which, as previously mentioned, cannot be carried by a membrane. Thus no calculations have been carried out for ρ_1 values below 0.1.

When s is determined, the slope φ is known from Eq. (5). The vertical displacement under the load can then be calculated by integrating the slope from the rim until the load radius (Table 2).

Maximum stress and deformation of the range $10^{-6}\leq 5\cdot 10^{-4}$ as thus calculated are shown in Figs. 2 and 3 by the points. The curves show the equations

$$\frac{w}{a}=f^{1/3}\cdot 0.158\left(\cot\frac{\pi}{1.1}\rho+0.94\sin\frac{\pi}{0.55}\rho+3.926\right)$$

$$s=f^{1/3}\cdot 0.862\left(1+0.8\cot\frac{\pi\rho}{1.41}\right)$$

These equations, which were evaluated as approximations for the result, thus appear to give quite a close coincidence. It should be noted that the proportionality to the powers ⅓ and ⅔ of f is in agreement with results for a distributed load.[1] As shown in Figs. 4 and 5, which give the same data as Figs. 2 and 3, the equations can, of course, be displayed as straight lines in a log-log diagram. The trigonometric functions, on the other hand, are just a trial-and-error fit, but apparently a successful one.

References

[1] den Hartog, J. P., *Advanced Strength of Materials*, McGraw-Hill, New York, 1952.

[2] Roark, R. J., *Formulas for Stress and Strain*, 4th ed., McGraw-Hill, New York, 1965.

Analytical Formulas for Conditions on Blunt Wedges in Hypersonic Flow

W. L. Bade*
Avco Systems Division, Wilmington, Mass.

Introduction

CHENG et al.[1] formulated an analytical theory of the combined effects of bluntness and boundary-layer displacement on the hypersonic flow over a wedge. Kemp[2] modified this analysis to include the effects of nonzero $(\lambda-)$ to first order. Boger and Aiello[3] generalized the theory to the case of nonzero yaw angle. The fundamental relation in the theory is the equation

$$(z-\Gamma\zeta)\frac{d}{d\zeta}\left(z\frac{dz}{d\zeta}\right)-\left(z\frac{dz}{d\zeta}\right)^{1/2}=J \tag{1}$$

in which z is a nondimensional variable proportional to the shock ordinate, ζ a nondimensional distance from the leading edge of the wedge, and Γ a constant parameter proportional to the angle of attack.

The boundary condition on Eq. (1) is $z=0$ at $\zeta=0$. The equation is singular at the origin. Sufficiently near the origin, the square root term and the term containing Γ can be neglected, and the equation admits a power-law solution $z=A\,\zeta^n$ with $n=2/3$, $A=(9/2)^{1/3}$. The solution for larger J can be generalized by numerical integration starting from a point on this singular solution.

For zero angle of attack, Eq. (1) has the analytical solution $z=z_0(\lambda)$, $\zeta=\zeta(\lambda)$, where

$$z_0(\lambda)=2[\tfrac{1}{3}\lambda^{3/2}-\tfrac{1}{2}\lambda+\lambda^{1/2}-\ln(1+\lambda^{1/2})] \tag{2a}$$

$$\zeta(\lambda)=\tfrac{1}{3}(1+\lambda^{1/2})^4-\frac{22}{9}(1+\lambda^{1/2})^3+9(1+\lambda^{1/2})^2-\frac{46}{3}(1+\lambda^{1/2})+\frac{10}{3}\ln(1+\lambda^{1/2})-4\lambda^{1/2}\ln(1+\lambda^{1/2})+2[\ln(1+\lambda^{1/2})]^2+\frac{76}{9} \tag{2b}$$

in terms of a parameter λ defined by

$$\lambda\equiv z\,dz/d\zeta \tag{3}$$

Received February 3, 1975; revision received March 10, 1975. This work was supported by NASA, Lyndon B. Johnson Space Center, under contract NAS9-9744.

Index categories: Rarefield Flows; Supersonic and Hypersonic Flow.

*Principal Staff Scientist.

For $\Gamma \neq 0$, the solution of Eq. (1) cannot be obtained in closed analytical form. The object of this Note is to present an analytical approximation to the solution for $\Gamma > 0$, and to show that the approximation has good physical accuracy over the entire range of conditions to which the theory is applicable for positive angle of attack.

Analytical Approximation to the Solution of the Wedge Equation for $\Gamma > 0$

The point symbols in Fig. 1 trace out solutions† of Eq. (1) for various values of Γ. For each Γ, the ordinate $(zz')' \equiv d(z\,dz/d\zeta)/d\zeta$ approaches the asymptotic value Γ^2 for $\zeta \to \infty$. For $\zeta \to 0$, each solution approaches the solution Eq. (2) for $\Gamma = 0$. These circumstances suggest that the solution for arbitrary Γ might be approximated by

$$(zz')' = ((zz')')_{\Gamma=0} + \Gamma^2 \tag{4}$$

where $[(zz')']$ is calculated from the solution (2) for zero angle of attack. From Eqs. (3) and (1) with $\Gamma = 0$

$$[(zz')']_{\Gamma=0} = \frac{1+\lambda^{1/2}}{z_0(\lambda)} \tag{5}$$

The curves in Fig. 1 represents Eq. (4). These curves were generated by choosing values of the parameter λ, calculating z_0 and ζ from Eq. (2) and $[(zz')']_{\Gamma=0}$ from Eq. (5), and then calculating $(zz')'$ for each Γ from Eq. (4).

The approximation Eq. (4) is most accurate from small Γ. For example, with $\Gamma = 0.1$, the maximum error is about 6%. Even for large Γ, the error in Eq. (4) is less than about 10% except in the region where $(zz')'$ is leveling off and beginning to approach its asymptotic value. In this region, for large Γ, the exact solution undershoots the asymptotic value and approaches it in an oscillatory manner. For $\Gamma = 100$, the difference between Eq. (4) and the exact solution becomes as large as a factor of 1.45 in this region.

However, Cheng et al.[1] suggest that the oscillations in the exact solution, which are responsible for these large differences, are unphysical artifacts of the system of approximations upon which the theory is based. If so, the approximate formula Eq. (4) might have higher physical accuracy than the exact solution. Comparisons with experimental data, presented following support this conjecture.

Comparisons with Experimental Data

The quantity $(zz')'$ in Eq. (4) is proportional to the surface pressure on the wedge. According to the theory,[3] the heat transfer coefficient is proportional to the quantity $(zz')'/(zz')^{1/2}$. From Eqs. (3) and (4),

$$zz' = \lambda + \Gamma^2 \zeta(\lambda) \tag{6}$$

The variable z itself, which is proportional to the shock ordinate, is given by a further integration

$$z = \{[z_0(\lambda)]^2 + \Gamma^2 [\zeta(\lambda)]^2\}^{1/2} \tag{7}$$

Figure 2 and 3 compare the approximate solution based on Eq. (4) with experimental data on the pressure and heat transfer distributions over the surface of a very blunt wedge in a hypersonic air stream. The experimental points are from Fig. 10 of Kemp's paper,[2] and are based on previously published data cited here. For a flow dominated by the effects of leading-edge bluntness, the nondimensional coordinate ζ is small, and the left-hand side of Eq. (1) is dominated by its first term, so that the solution for $\Gamma = 0$ is[3]

$$z_0 \simeq (9/2)^{1/3} \zeta^{2/3} \tag{8}$$

†These numerical solutions were computed by R.C. Boger, AVCO Systems Division.

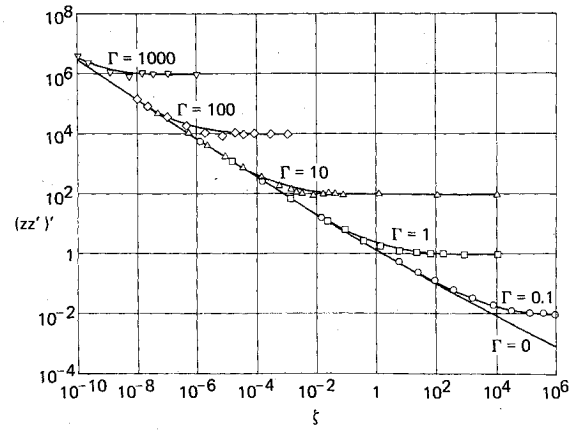

Fig. 1 Solutions of the equation for flow over a wedge (points —exact numerical solutions; curves—analytical approximation).

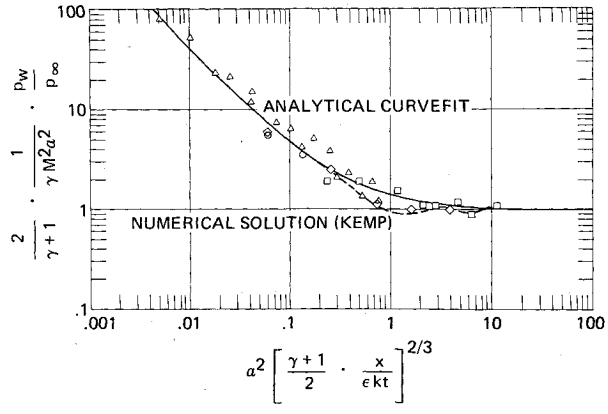

Fig. 2 Pressure on a very blunt wedge (solid curve—analytical approximation; dashed curve—exact solution; points—experimental data).

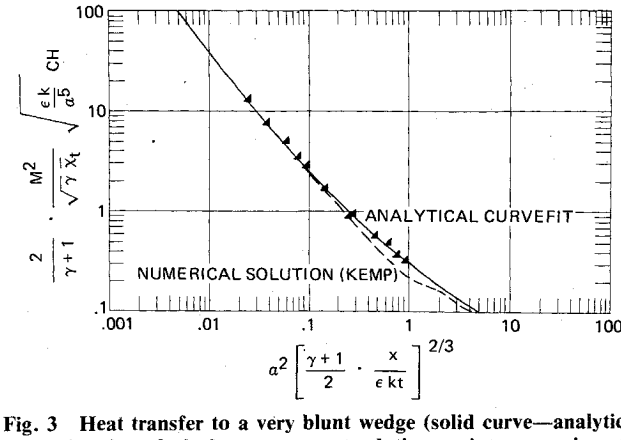

Fig. 3 Heat transfer to a very blunt wedge (solid curve—analytical approximation; dashed curves—exact solution; points—experimental data).

Equation (4) then gives, for $\Gamma > 0$

$$(zz')' \simeq (2/9)^{1/3} \zeta^{-2/3} + \Gamma^2 \tag{9a}$$

$$zz' \simeq 6^{1/3} \zeta^{1/3} + \Gamma^2 \zeta \tag{9b}$$

Substitution of these formulas into the expressions[3] for the pressure and heat transfer coefficient in terms of the nondimensional variables gives

$$\frac{2}{\gamma+1} \cdot \frac{1}{\gamma M^2 \alpha^2} \cdot \frac{p_w}{p_\infty} = 1 + \frac{0.382}{\xi} \tag{10a}$$

$$\frac{2}{\gamma+1}\cdot\frac{1}{\gamma^{1/2}}\cdot\frac{M^2}{\bar{\chi}_t}\left(\frac{\epsilon k}{\alpha^5}\right)^{1/2}C_H = \frac{0.332(1+0.382/\xi)}{\xi^{1/4}(1.145+\xi)^{1/2}} \quad (10b)$$

where

$$\xi \equiv \alpha^2\left(\frac{\gamma+1}{2}\cdot\frac{x}{\epsilon k t}\right)^{2/3} \quad (11)$$

The notation is as defined by Kemp.[2] The unbroken curves in Figs. 2 and 3 represent Eqs. (10a) and (10b), respectively. The agreement with the experimental data is similar to that shown in Kemp's[2] original Fig. 10. In the region $\xi \simeq 1$, where the pressure curve in Fig. 2 is leveling out, the agreement in both pressure and heat transfer is better than is obtained with the exact solution of the Cheng equation (shown by the dashed curves in Figs. 2 and 3).

References

[1] Cheng, H. K. Hall, G. J., Golian, T. C., and Hertzberg, A., "Boundary-Layer Displacement and Leading-Edge Bluntness Effects in High-Temperature Hypersonic Flow," *Journal of Aerospace Science*, Vol. 28, May 1961, pp. 353-381; Errata in Vol. 29, March 1962, p. 355.

[2] Kemp, J. H. Jr., "Hypersonic Viscous Interaction on Sharp and Blunt Inclined Plates," *AIAA Journal*, Vol. 7, July 1969, pp. 1280-1289.

[3] Boger, R. C. and Aiello, G. F., "Hypersonic Flow on Yawed Wedges with Leading-Edge Bluntness and Viscous Interaction," *Journal of Spacecraft and Rockets*, Vol. 8, July 1971, pp. 729-735.

Boundary-Layer Effect in Panel Flutter

Marvin E. Goldstein*
NASA Lewis Research Center, Cleveland, Ohio

Nomenclature

$a(y)$ = speed of sound nondimensionalized by a_∞
a_∞ = speed of sound in mainstream
$A_\pm$ = defined by Eq. (20)
b = $k^2/2ik_1M_\infty U'$
$B_\pm^{(r)}$ = defined by Eq. (21)
$C_\pm, C_0$ = arbitrary constants
d = plate semi-length
$\hat{\imath}$ = unit vector in x-direction
$\hat{k}$ = unit vector in z-direction
$\boldsymbol{k}$ = $\hat{\imath}k_1+\hat{k}k_3$ wave number vector
k_1 = wave number in x-direction
k_3 = wave number in z-direction
k = $|\boldsymbol{k}|$
K = defined by Eq. (23)
M_∞ = freestream Mach number $U_\infty/a_\infty > 1$
$\mathfrak{M}$ = $M_\infty[(\omega/k_1)-U]/a$
p = pressure fluctuation
P = Fourier transfer of p
t = time, nondimensionalized by U_∞/d
$U(y)$ = mean boundary layer velocity at y
U_p = $U(\bar{y}_p)$
U_∞ = mean velocity in mainstream
w_p = plate deflection
W_p = Fourier transform of w_p
x,y,z = spatial coordinates nondimensionalized by $d/2$
$\bar{y}_p$ = effective mean wall position
α = $[2iM_\infty/(U'k_1)]^{1/2}$
∇ = gradient operator
β = $[M_\infty^2(\omega-k_1)^2-k^2]^{1/2}$
γ = ratio of specific heats
Γ = defined in Eq. (12)
δ = $\Delta/(d/2)$
Δ = boundary-layer thickness
ξ = $[2ik_1/(U'M_\infty]^{1/2}$
$\bar{\rho}_p$ = average density at plate
ω = dimensionless frequency

Received March 7, 1975; revision received April 11, 1975.
Index categories: Nonsteady Aerodynamics; Aircraft Vibration; Aircraft Structural Design.
*Research Scientist. Member AIAA.

Introduction

As pointed out by Dowell,[1] it is now firmly established that the adjacent boundary layer will have an important influence of the flutter behavior of plates. This effect has been considered by a number of investigators.[1-3] An important part of the problem (the aerodynamic part) is the determination of the relation between the fluctuating force exerted by the flow on the panel and the transverse displacement of the panel. (This relation is frequently expressed as a "generalized aerodynamic force.") It usually is necessary to determine the resulting force numerically.[1-3] In this Note we shall show that if the supersonic Mach number of the stream is not too large, an analytical expression can be obtained for this force. The low supersonic Mach numbers are the ones of maximum interest in the present problem because it is in this Mach number region where the boundary layer has the most influence. For example, Dowell[1] shows that the presence of the boundary layer causes about a 300% increase in flutter dynamic pressure at a Mach number of about 1.2, while it causes only about a 20% increase at a Mach number of 2.

Analysis

The configuration of interest is shown in Fig. 1. It can be shown by rearranging Eq. (18) of Ref. 1 that the pressure fluctuations in the boundary layer caused by the motion of the panel is governed by the equation

$$\frac{\mathrm{d}}{\mathrm{d}t}\left[\frac{1}{a^2}\nabla\cdot(a^2\nabla p)-\frac{M_\infty^2}{a^2}\frac{\mathrm{d}^2}{\mathrm{d}t^2}p\right]-2U'\frac{\partial^2 p}{\partial x\partial y}=0 \quad (1)$$

where all lengths are nondimensionalized by the panel half length d, the time t is nondimensionalized by U_∞/d, the mean velocity is nondimensionalized by U_∞, the speed of sound is nondimensionalized by a_∞,

$$(D/Dt) \equiv (\partial/\partial t)+U(\partial/\partial x) \quad (2)$$

and the prime denotes differentiation with respect to y.

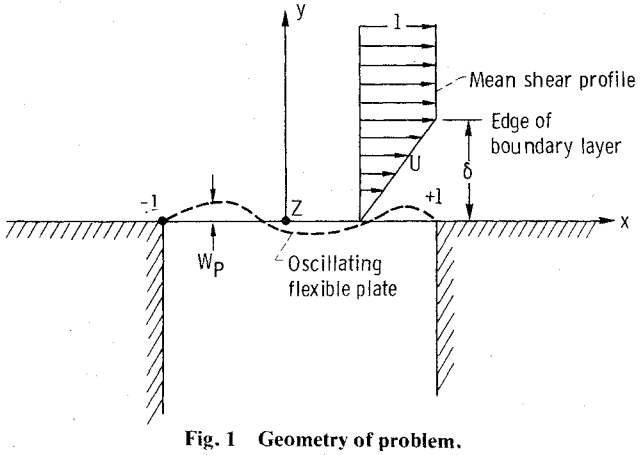

Fig. 1 Geometry of problem.